Biomedical Signal Processing and Control 83 (2023) 104711

Contents lists available at ScienceDirect

Biomedical Signal Processing and Control

journal homepage: www.elsevier.com/locate/bspc

Nearly-lossless-to-lossy medical image compression by the optimized JPEGXT and JPEG algorithms through the anatomical regions of interest

Zhongqiang Li [a], Alexandra Ramos [b], Zheng Li [a], Michelle L. Osborn [b], Waleed Zaid [c], Xin Li [e], Yanping Li [d], Jian Xu [a,*]

[a] Division of Electrical and Computer Engineering, College of Engineering, Louisiana State University, Baton Rouge, LA 70803, USA
[b] Department of Comparative Biomedical Science, School of Veterinary Medicine, Louisiana State University, Baton Rouge, LA 70803, USA
[c] Oral and Maxillofacial Surgery, School of Dentistry, Louisiana State University Health Science Center, Baton Rouge, LA 70808, USA
[d] School of Environment and Sustainability, University of Saskatchewan, Saskatoon, SK S7N 5C9, Canada
[e] School of Performance, Visualization, & Fine Art and Aggie Computer Graphics Group, Texas A & M University, College Station, TX 77843, USA

ARTICLE INFO

Keywords:
Medical image compression
Region of interest
JPEGXT_OPT
JPEG_OPT
Nearly-lossless and lossy compression

ABSTRACT

Currently, plenty of image data is generated that complicate storage and image transmission. Great efforts have been attempted on how to increase compression ratio (CR) without loss of critical diagnostic information. In this study, we designed two optimized JPEGXT (JPEGXT_OPT) and JPEG (JPEG_OPT) approaches by amplifying discrete cosine transform coefficients and using the entire anatomical region as ROI (region of interest). We found that ROI percentages have a great impact CR: smaller ROI percentages (10–30 %) could obtain a larger CR. Under the near-lossless compression, JPEGXT_OPT could have CRs up to 4.0 under small ROI percentages (10–30 %), while only ~ 1.2 for large ROI percentages (90–100 %). JPEG_OPT could obtain a much higher CR: up to over 20.0 for both CT and MRI images under small ROI percentages (10 %-30 %), and over 10.0 in CT and 5.0 in MRI under large ROI percentages (90 %). Both of them show a compression efficiency than the DICOM-recommended JPEGXT and JEPG_2000. From the distortion analysis, MSSIM (Multiscale Structural Similarity) and PRD (percent ratio of distortion) indicate our methods have a less image distortion than DICOM-recommended JPEGXT (PDR > 20 %) and JPEG_2000: approximately 3.0 % PRD were seen under JPEG_OPT, while<0.15 % PRD were observed under JPEGXT_OPT. MSSIM > 0.98 was found in JPEG_OPT, which the reconstructed images have almost no changes in luminance, contrast, and structure, and this was confirmed by low PRD (about 3.0 %). Overall, our two methods could provide a high compression ratio of medical images without significant loss of important diagnostic information in reconstructed images.

1. Introduction

To date, medical imaging has significant uses in both clinics and research, and many medical techniques are becoming digital formats [1–4]. The large amount of image data generated by imaging techniques, notably computed tomography (CT) and magnetic resonance images (MRI), presents challenges in data storage, image processing, and image transmission [5–9]. In particular, the Picture Archiving and Communication Systems (PACS), the most common archiving and communication system used in clinics, requires higher speed and broader bandwidth for the transmission of vast amounts of medical image data [2,10]. Thus, decreasing the size of image data will save storage space, image transfer time, and medical cost [11–14].

Compression techniques that reduce the size of image data could help to solve the problems of image transmission and storage [15]. Lossless algorithms could compress and reconstruct medical images without losing any information of the original image, but their current compression ratio is limited to 2.0 to 3.0 depending on the images and the methods used [16]. To further improve the compression ratio, a more practical method for lossless approaches is to remove data of unimportant areas outside regions of interest (ROI) in medical images [17]. Image segmentation is the key step to extracting ROI from the whole image, and ROI boundaries can be determined by an automatic or semi-automatic process [7]. However, complicated ROI (especially ROI related to diseased areas) must be specified interactively by specialists or technicians who are skilled in profiling the critical diagnostic

* Corresponding author.
E-mail address: jianxu1@lsu.edu (J. Xu).

https://doi.org/10.1016/j.bspc.2023.104711
Received 5 May 2021; Received in revised form 26 November 2022; Accepted 11 February 2023

information from the whole images [18].

Lossy techniques obtain much higher compression ratios (over 10.0, saving about 90 % of storage) than lossless compression [16]. To date, many algorithms have been developed for image compression, and one of the most frequently utilized is JPEG [19], and the most common standards include baseline JPEG [2,20], JPEG-2000 [2], JPEG-LS [2,12], and JPEGXT [2,21], and so on. Until now, lossy approaches are not well accepted in the medical imaging field, because of concerns about losing critical changes in medical images [19,22]. However, if the image distortion could be controlled within a certain level, the lossy algorithms could allow being used in medical images [5]. Several professional societies have given guidelines or recommendations of compression ratio for the use of lossy algorithms in medical images [2,23,24]. In particular, the latest DICOM (Digital Imaging and Communications in Medicine) protocols have provided the guidelines to support the use of JPEG-based approaches (such as JPEG, JPEG 2000, JPEGXT, and so on) for the compression of medical images [25].

In addition, more and more novel compression algorithms, as well as ROI-based approaches, are being developed, but most of the existing studies only used limited number of medical images to test the efficiency of the algorithms [14,16,26–29]. To our best knowledge, few studies have systematically reported how the area of anatomical regions occupied in the entire image effect the compression ratio. Even though the recommended compression ratio has been given by professional organizations, their guidelines did not show how this value was obtained or whether different areas of anatomical regions would impact the recommended compression ratio or not [23,24]. Meanwhile, JPEG still serves as one of the most widely used image compression and the most common digital image format, but JPEG still could not be used to compress medical images with>8-bit depth [2,30].

Therefore, this study uses the anatomical regions in medical images as ROI to further optimize the compression ratio of our previous JPEGXT_OPT algorithm and investigate the influences of ROI percentages occupying in whole images on compression ratio [21]. We also developed an optimized JPEG (JPEG_OPT) method to increase compression ratio and better compression quality for 16-bit depth CT and MRI images by amplifying DCT (discrete cosine transform) coefficients. We also further compared their compression efficiency with the DICOM-recommended JPEGXT (JPEGXT_T) and JPEG_2000.

2. Materials and methods

2.1. CT and MRI datasets

In this study, 4211 medical images (including 2478 CT images and 1733 MRI images) with the dimension of 515*512 were employed to investigate the efficiency of ROI-based JPEGXT-OPT and JPEG_OPT for the compression of 16-bit depth medical images. Those CT and MRI images were obtained from Cancer Imaging Archive [31,32], the file format of the imaging dataset was *. *dcm*, and most of the imaging parts in the CT and MRI dataset were from brain, head, chest, and so on.

2.2. Optimized JPEG-based algorithm for the high-compression of medical images

In our previous study, we found that the lower 8-bit subimages occupied most of the storage space in the encoding files [21]. To further increase the compression ratio and avoid the influence of the lower 8-bit subimages, the original medical image (ORG, PXL_{ORG} ranges: 0–65535) was converted into a new 8-bit medical image (New_PXL ranges: 0–255) by using the following equation (1):

$$New\_PXL = \frac{255^{*}PXL_{ORG}}{PXL_{ORG\_max} - PXL_{ORG\_min}} \quad (1)$$

PXL_{ORG} is the pixel values in the original medical image;

PXL_{ORG_max} is the maximum pixel values in the original medical image;

PXL_{ORG_min} is the minimum pixel values in the original medical image.

2.3. ROI-based JPEGXT-OPT for the compression of CT and MRI images

Fig. 1 illustrates the flowchart of ROI-based JPEGXT_OPT for the compression of CT and MRI images. First, the maximum pixel was found from the input 16 bit-depth images. Second, the input 16-bit depth image was binarized based on the anatomical regions; the boundaries of anatomical regions were determined by a threshold of the maximum pixels: if the maximum pixel is smaller than the threshold (4100 for CT images and 10,000 for MRI images), all the pixels with larger than H_% (high_percentage: CT: 20 %, MRI: 10 %, determined by the maximum pixels and background pixels, as shown in Fig. S1) of the maximum pixels were reset at 1, while the rest of the pixels were set to 0. But if the maximum pixel is larger than the threshold, the pixels larger than L_% (low percentage: CT and MRI: 3 %, determined by the maximum pixels and background pixels, as shown in Fig. S1) of the maximum pixels were set at 1, and the rest pixels were set at 0. After that, the input CT or MRI images were binarized, and the anatomical regions had pixel values equal to 1, while 0 for the background pixels.

Third, because most of the anatomical structures concentrate in one region, ROI could be determined by the largest connected components in the binarized images. Then, two types of ROI regions were tested in this study: one is the cropped ROI regions (ROI_REGN) as the input (used in JPEG_OPT); the other is only the ROI pixel (ROI_PXLs) list as the input. For the first input, the ROI regions simply were cropped from the original CT and MRI images by using the minimum and maximum coordinate points, and the minimum coordinate points were stored into the compression codes to recover the ROI region into the reconstructed images.

However, there were still some background pixels that were also cropped into the ROI regions. To remove the extra background, the pixel values of the ROI_PXLs list were reshaped as an 8*m ROI_PXLs IMG (m is the number of columns) so the reshaped image be compressed by JPEG-based algorithms. Then, this reshaped 8*m ROI_PXLs image is used as the input of JPEGXT_OPT method; its two coordinate lists were directly stored into the encode files to recover ROI pixels in the reconstructed images.

Finally, two types of ROI inputs were loaded into JPEGXT_OPT and JPEG_OPT algorithms; the JPEGXT_OPT would split the input 16-bit depth medical image into an upper 8-bit (9th −16th bits) subimage and a lower 8-bit (1st −8th bits) subimage [21]. In our previous study, we found that the upper 8-bit subimages has a more important role in the improvement of medical compression than lower 8-bit subimages; N = 20 (N: discrete cosine transform amplifying coefficient) and NDP = 1 (NDP: Number of Decimal Portions) in lower subimages and lossless compression (N = 400, and NDP = 2) in upper subimages could achieve a similar compression quality with JPEG-2000[21]. Thus, this study uses HQ (high quality, N = 100, NDP = 1: JPEGXT_OPT HQ) compression and LQ (N = 10, NDP = 1: JPEGXT_OPT LQ) compression in lower 8-bit subimages to explore the efficiency of ROI-based JPEGXT_OPT.

For the JPEG_OPT, ROI_REGN images use HQ (N = 400, NDP = 2: JPEG_OPT HQ) compression and LQ (N = 10 for CT and N = 50 for MRI, NDP = 1: JPEG_OPT LQ) compression in the new ROI_REGN images to explore the efficiency of ROI-based JPEGXT_OPT.

2.4. Evaluation of compression efficiency

To investigate the influence of ROI percentage on the compression ratio, we calculated the corresponding percentages through formula in each CT and MRI image (2):

$$ROI\_Percentage = \frac{PXL_{ROI}NUM}{PXL_{ORG}NUM} \quad (2)$$

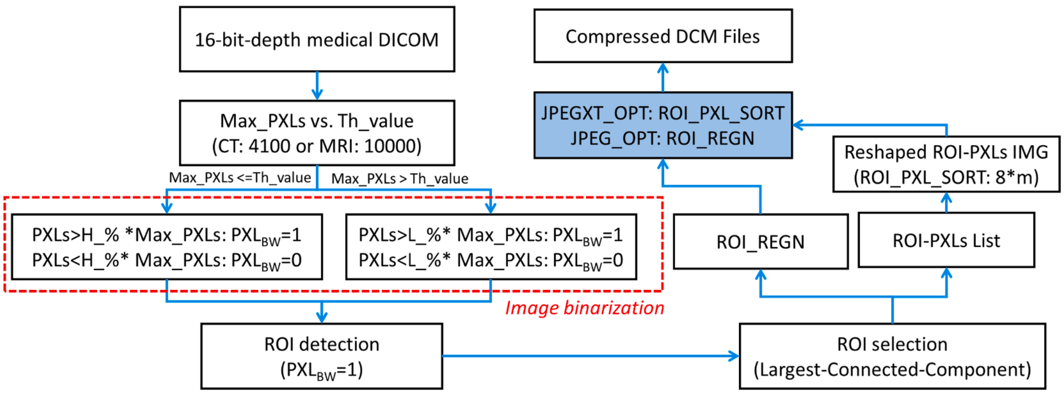

Fig. 1. The flowchart of ROI-based JPEGXT_OPT algorithm for the compression of 16-bit depth medical images.

$PXL_{ROI}\,NUM$ is the number of pixels in the ROI;

$PXL_{ORG}\,NUM$ is the number of pixels in the original medical images.

In image compression, Peak-Signal-to-Noise ratio (PSNR), Mean Square Error ratio (MSE), and the Compression ratio (CR) are the most common parameters to evaluate the compression efficiency [33]. PSNR, MSE, and CR could be obtained from:

$$MSE = \frac{\sum_{m,n}(I_{ORG}(m,n) - I_{RECOV}(m,n))^2}{m^*n} \tag{2}$$

$$PSNR = 10^*\log_{10}\left(\frac{R^2}{MSE}\right) \tag{3}$$

$I_{\mathrm{ORG}}(m,n)$ is the original medical image;

$I_{\mathrm{RECOV}}(m,n)$ is the reconstructed medical image;

m,n is the dimension of the two input images;

R is the maximum fluctuation in medical images (e.g. 65,535 for 16-bit medical images).

$$CR = \frac{Uncompressedsize}{Compressedsize} \tag{4}$$

Uncompressedsize is the file sizes of the original medical image;

Compressedsize is the encoded files of the original medical images.

2.5. Evaluation of image distortion between original and reconstructed medical images

MSSIM (Multiscale Structural Similarity) is an optimized parameter based on the SSIM (Structural Similarity). SSIM could extract structural information from the images, but only evaluate the image quality from the single scale [34]. However, MSSIM could provide a more accurate assessment of image quality, because it can analyze the spatial resolutions from different scales of SSIM components, such as luminance, contrast, and structures[34,35].

The percentage of distortion (PRD) is to evaluate the distortions in the reconstructed image relative to the original medical image; smaller PRDs mean fewer distortions in the reconstructed images [28].

$$PRD = 100^*\sqrt{\frac{\sum_{x=1}^{m}\sum_{y=1}^{n}[I_{ORG}(x,y) - I_{RECOV}(x,y)]}{\sum_{x=1}^{m}\sum_{y=1}^{n}[I_{ORG}(x,y)]^2}} \tag{5}$$

$I_{\mathrm{ORG}}(x,y)$ is the pixel of the original medical image;

$I_{\mathrm{RECOV}}(x,y)$ is the pixels of the reconstructed medical image;

All the codes of the algorithms were performed in Matlab 2019a (MathWorks Inc, Natick, Mass).

3. Results

3.1. Distribution of ROI percentages in the CT and MRI image datasets

From Fig. S1, the means of ROI regions was much larger than the BG (background) pixels: the means of ROI pixels were around 1000 in CT and 2000 in MRI, while BG had only about 50 in CT and 100 in MRI images, which the BG means were about 20 times lower than ROI pixels in both CT and MRI. In this case, there were cut-off lines that could be found to distinguish ROI and BG. However, in this study we found different CT and MRI images have great changes in pixels, especially the maximum pixels (as shown in Fig. 2c). Thus, it is very difficult to find a uniform percentage for all of CT and MRI images.

For instance, two CT images with a large maximum pixel (32767, due to amalgam fillings in tooth) and a small maximum pixel (1084) were shown in Fig. 2. For the large maximum pixel, the large maximum pixel value is usually from the metal implants in the patient's tooth (Fig. 2a). When the H_% threshold was set at a large threshold percentage (20 %) of the maximum pixel, only a few areas around the maximum pixel could be selected; most of the anatomical regions were missing. However, if this threshold percentage was decreased to 3 %, then the entire anatomical regions (ROI) could be accurately profiled in the binarized CT image (Fig. 2a). On the contrary, in the CT image with small maximum pixels, the small threshold percentage (3 %) of the maximum pixels would cause over cropping of the anatomical regions (ROI), but it could be successfully detected if the threshold percentage was set at 20 % of the maximum pixels (Fig. 2b). Thus, this study we used different H_% and L_% for the CT and MRI images with different maximum pixels.

From the maximum pixel curves of all the CT images (sorting based on the maximum pixel from the largest to the smallest), the maximum pixel had a rapid decrease from 32,767 to around 4100, and then the rest of the maximum pixel narrow at the ranges between 1000 and 4100 (Fig. 2c). Thus, 4100 seems to be the threshold of the CT maximum pixels that the percentage should be set at 20 % for the maximum pixels<4100 and 3 % for the maximum pixel above 4100. For the MRI images, we found that this threshold of the maximum pixels should be set at around 10,000 to obtain the accurate anatomical regions (Fig. 2c).

Fig. S1 indicated that compared to ROI pixels, BG regions had more stable distributions, and most of BG pixel means in both CT and MRI images only distribute within the small ranges (seen the distributions of error bars in Fig. S1c and S1d). For the maximum pixels larger than Th_value, smaller percentage (L_%) should be used to cover whole ROIs (like Fig. 2a), when maximum pixels smaller than Th_value, we have to increase the percentage (H_%) to avoid overcropping BG regions (like Fig. 2b). In addition, the cut-off lines had a similar distribution with ROI pixel means and well located between BG and ROI mean curves. From the distributions of error bars in ROI and BG mean curves, most of cut-off lines, especially 20 % in CT and 10 % in MRI for the maximum pixels smaller than Th_value, distributed under lower error bars of ROI or

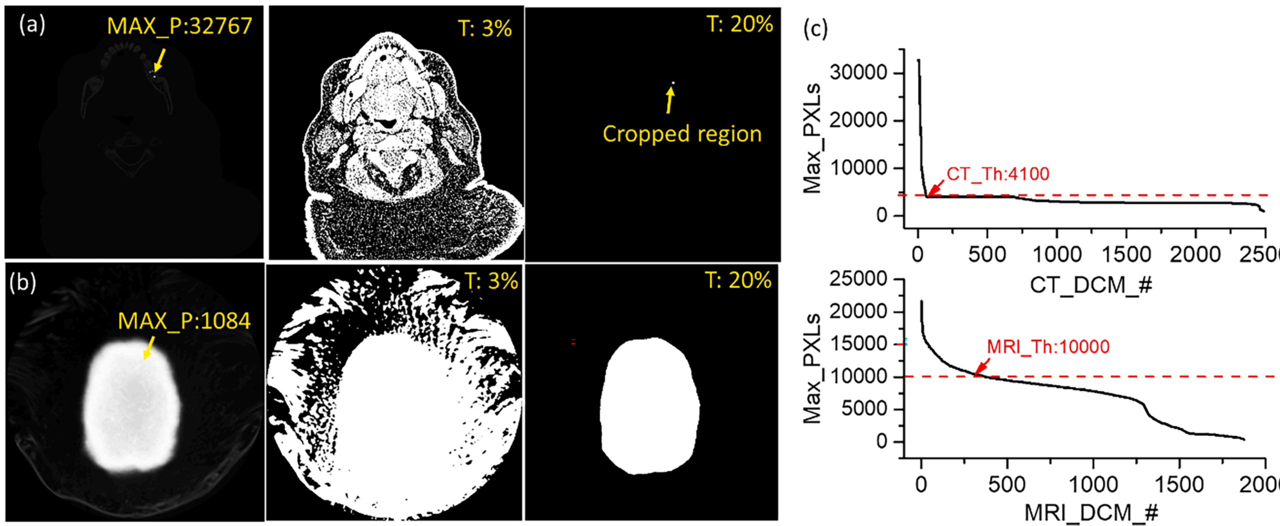

Fig. 2. ROI region detection based on the thresholds of the maximum pixels. (a) ROI detection in large maximum pixel values; (b) ROI detection in small maximum pixel values; (c) The maximum pixel distributions in the CT and MRI images.

above the upper error bars of BG regions, which means cut-off boundaries could distinguish ROI and BG regions (Fig. S1c and S1d).

After determining the threshold and corresponding percentages of the maximum pixels, the CT and MRI images were cropped to obtain the ROI regions, and then the ROI percentages were calculated for all the CT and MRI datasets. From the proportional distributions in Fig. 3, both CT and MRI had the largest proportion (over 40 %) of images with ROI percentages between 50 and 70 %, followed by the ROI percentages around 30–50 %. Overall, almost over 70 % of CT images and 90 % of MRI images had ROI percentages<70 % of the entire medical images, which means the rest of the background regions (>30 %) did not contain any useful information.

3.2. ROI_PXL_SORT for nearly-lossless compression of CT and MRI images

A CT image (Fig. 4) was used to show the difference between ROI_PXL_SORT and ROI_REGN. The binarized images indicate the entire anatomical ROI could be correctly profiled by using our method (Fig. 4a and 4b). From ROI_REGN, if ROI was directly cropped from the whole medical images, parts of the background regions (BG regions in Fig. 4c) were cropped within ROI, which would cause a decrease in compression ratio. However, if only using ROI pixels with their coordinates, those BG regions could be removed (Fig. 4d).

ROI_REGN or ROI_PXL (without resorting) were directly compressed by JPEGXT_OPT LQ, the reconstructed ROI image had lower PSNR (<80 dB) and larger MSE (>40) when compared to the ORG (original image) compression (>80 dB and MSE < 4) (Fig. S2). But ROI_PXL_SORT could achieve a similar compression quality to ORG compression with HQ compression (Fig. S3).

Regarding compression ratio under different ROI percentages, under the same ROI percentage, the larger N value (JPEGXT_OPT HQ) would decrease almost half of CR in the ORG compression than the lower N value (JPEGXT_OPT LQ), especially in CT. For ROI_PXL_SORT, it could have a larger CR (>4.0) under small ROI percentages (<30 % in CT and MRI); higher CR could be obtained by ROI_PXL_SORT than ORG compression under JPEGXT_OPT HQ, but under JPEGXT_OPT LQ it became opposed at ROI percentages was ranging from 30 % to 100 % (Fig. 5).

For the relationship between CR and ROI percentages, ROI percentages affected the compression ratio in both ORG and ROI_PXL_SORT; smaller ROI percentages had larger CRs, especially ROI_PXL_SORT could achieve CR over 4.0 under small ROI percentages (<30 %), which could save about 75 % of storage spaces (Fig. 5). For the ROI percentage ranges from 30 % to 90 %, ROI_PXL_SORT with LQ compression (N = 10) could still obtain large CR (around 2.0 if ROI percentages < 70 %). For ROI percentage > 90 %, JPEGXT_OPT HQ with ORG compression had a relatively larger CR (~1.4, saving about 30 % of storage space) than ROI_PXL_SORT (CR = 1.1, only saving about 10 % of storage space). Thus, within a small ROI percentage (10 %),

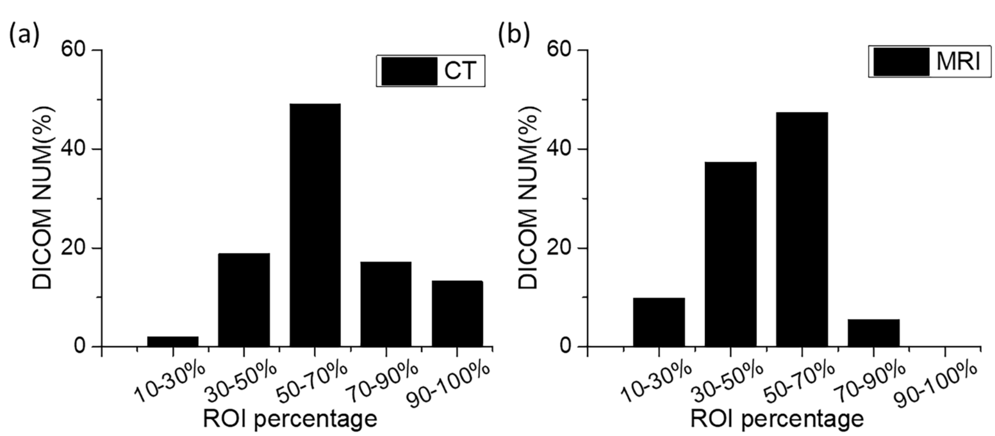

Fig. 3. The proportional distributions of (a) CT and (b) MRI images under different ROI percentages.

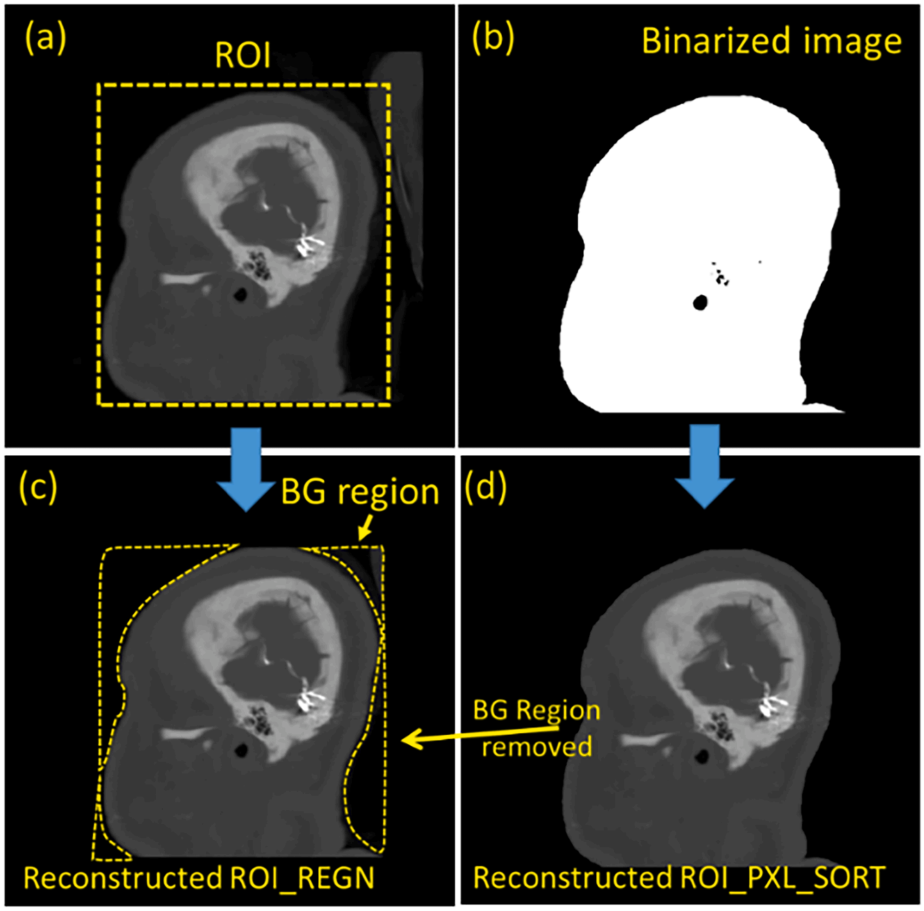

Fig. 4. Reconstructed images based on ROI-based JPEGXT_OPT methods. (a) Original image; (b) Binarized image; (c) Reconstructed image from ROI_REGN methods, (d) Reconstructed image from ROI_PXL_SORT method. BG: background (not anatomical regions).

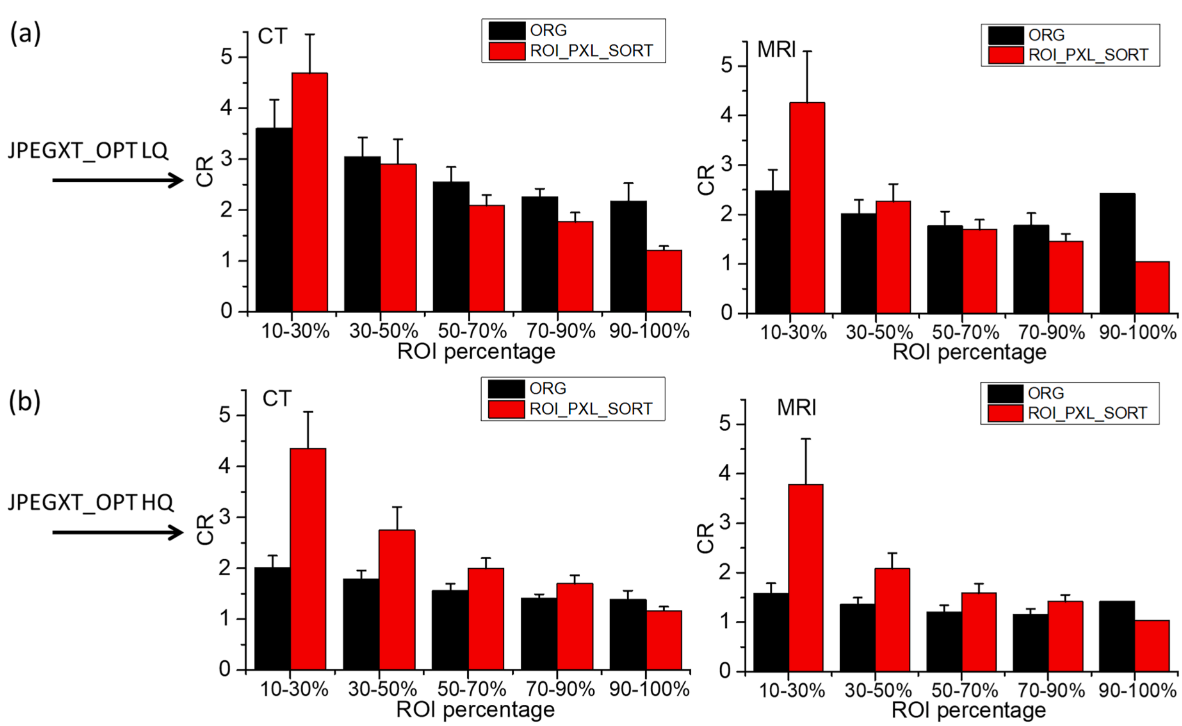

Fig. 5. CR distributions under different ROI percentages between ORG compression and ROI_PXL_SORT by using JPEGXT_OPT. (a) JPEGXT_OPT LQ; (b) JPEGXT_OPT HQ.

ROI_PXL_SORT with LQ compression could be employed, while for a large ROI percentage (90–100 %) the whole medical images could be compressed by JPEGXT_OPT HQ (Fig. 5).

Compared to the DICOM-recommended algorithms: JPEGXT_T (PSNR < 60 and MSE > 1200) and JPEG_2000 (PSNR < 80 and MSE > 20), JPEGXT_OPT had a larger PSNR (about 90 dB) and smaller MSE (<4.0) in the compression of the original images (ORG) (Fig. 6). Compared to ORG compression, ROI_PXL-SORT could help to improve the compression efficiency not only in JPEG_OPT but also in the DICOM-recommended methods (JPEGXT_T and JPEG_2000); but JPEGXT_OPT still show the best compression efficiency (PSNR > 105.0 dB and MSE < 0.2), followed by JPEG_2000 (PSNR < 100.0 dB and MSE > 0.4), when JPEGXT_T had the lowest PSNR (<80 dB) and largest MSE (>20.0) (Fig. 6).

In ORG compression, JPEGXT_OPT had the lowest compression ratio (only around 2.5 for CT and 2.0 for MRI), which was much lower than the DICOM-recommended methods: JPEGXT_T and JPEG_2000 (CR > 5.0). Although ROI_PXL_SORT could greatly improve PSNR and MSE for the DICOM-recommended methods, their compression ratio had also a big decrease (drop to around 2.0). JPEGXT_OPT almost had no change in the CR of the entire image datasets between ORG and ROI_PXL_SORT, but ROI_PXL_SORT method could help to greatly increase CR under small ROI percentage or HQ compression (Fig. 5).

3.3. JPEG-OPT approach for high compression-ratio of medical images

In the JPEGXT_OPT with ROI_REGN, it had relatively low compression quality (PSNR < 80 and MSE > 40) in both CT and MRI images, when compared to the JPEGXT_OPT with ORG and ROI_PXL (Fig. S2). However, if ROI regions are added with additional 8-pixel-width edges (Fig. 7), both PSNR and MSE could be improved, although CR even had slight decreases in both CT and MRI (Fig. S4).

In our previous study, we found the lower 8-bit encoding files occupied over 90 % of the storage space [21]. To further increase the compression ratio and avoid the impact of lower 8-bit encoding files, this study further developed a JPEG_OPT algorithm based on JPEGXT_OPT. In this approach, 16-bit depth medical images were converted into 8-bit depth images, and then the new 8-bit depth images were compressed by JPEG_OPT. Similar to JPEGXT_OPT, the compression quality could be adjusted by changing N and NDP values.

From ROI_REGN_EDG-based compression, the best compression quality was found in JPEGXT_OPT LQ, but JPEG_OPT could still achieve efficient compression quality (PSNR > 80 and MSE < 50). Compared to DICOM-recommended methods: JPEGXT_T (PSNR = 60, MSE > 2000) and JPEG_2000 (PSNR = 78, MSE < 50.0), JPEG_OPT with HQ compression showed better PSNR and MSE. For JPEG_OPT LQ, although its PSNR was similar to JPEG_2000 and MSE was a little larger than JPEG_2000, it had a much larger compression ratio (CR up to 13.0 in CT and 7.0 in MRI) than JPEG_2000 (about 2.0 lower) (Fig. 8).

Regarding CR distributions under different ROI percentages, Fig. 9 indicates that JPEG_OPT LQ with ROI_REGN-EDG had over 10.0 of CRs (saving over 90 % of storage spaces) under the whole range of ROI percentages (10 %-100 %) in CT images, which was higher than JPEGXT_T and JPEG_2000. For MRI images, JPEG_OPT_LQ had larger CRs (CR > 7.0, saving about over 85 % of storage space) than JPEG_2000 for ROI percentages < 70 %, and CR became smaller than JPEG_2000 for the rest of ROI percentages (Fig. 9). Although larger CR was found in JPEGXT_T than in JPEG_OPT_LQ, it had much larger PSNR and MSE than JPEG_OPT and JPEG_2000.

For the JPEG_OPT_HQ and JPEGXT_OPT, we could see that JPEG_OPT_HQ had larger CRs than JPEGXT_OPT under the small ROI percentages (<60 % for CT and < 80 % for MRI). Since they had better compression quality (large PSNR and low MSE), those two methods still could achieve over 3.0 CR efficiency. However, compared to the ROI-based method, a much lower compression ratio (decreasing about 5.0) could be found in ORG compression, especially under smaller ROI percentages (Fig. S6).

3.4. Evaluate the distortion of reconstructed images by JPEGXT_OPT and JPEG_OPT approaches

From the MSSIM evaluation, JPEGXT_OPT with both HQ and LQ

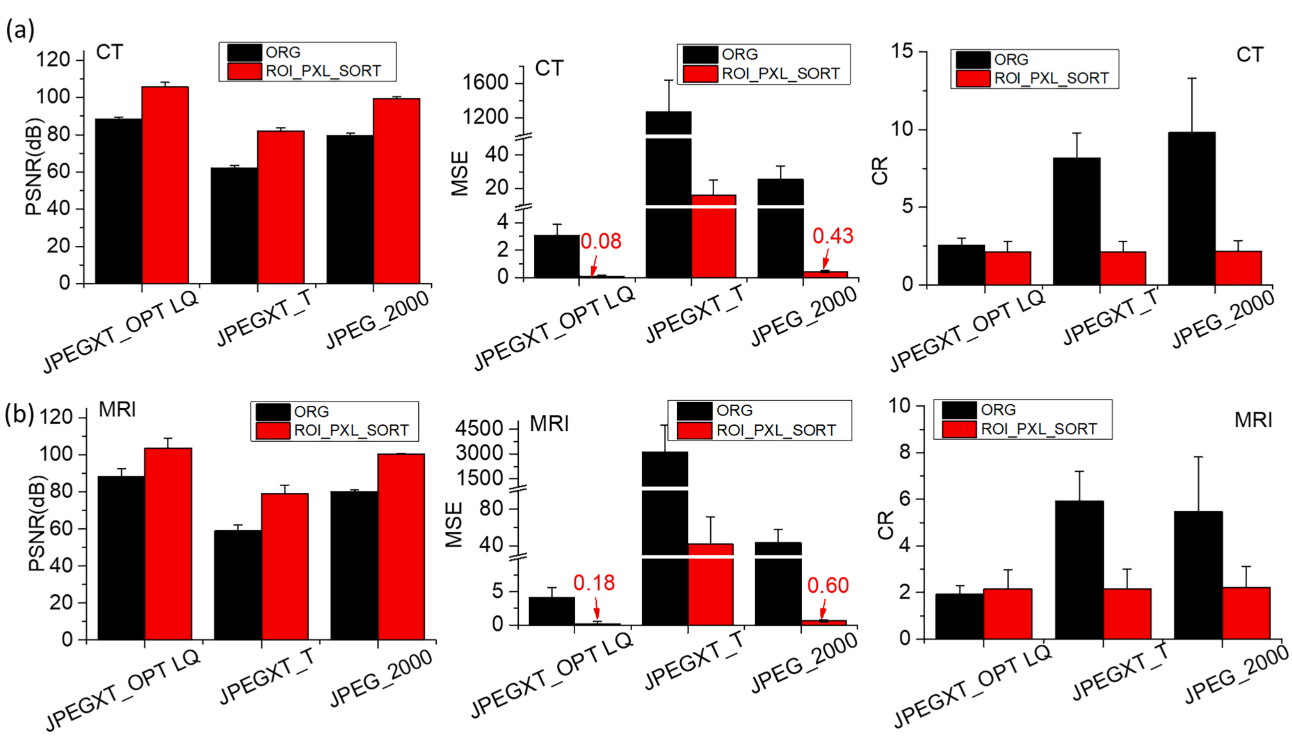

Fig. 6. Evaluation of the ORG and ROI_PXL_SORT compression of CT and MRI images by using JPEGXT_OPT LQ, and the DICOM-recommended methods: JPEGXT_T, and JPEG_2000. (a) PSNR, MSE, and CR in CT; (b) PSNR, MSE, and CR in MRI.

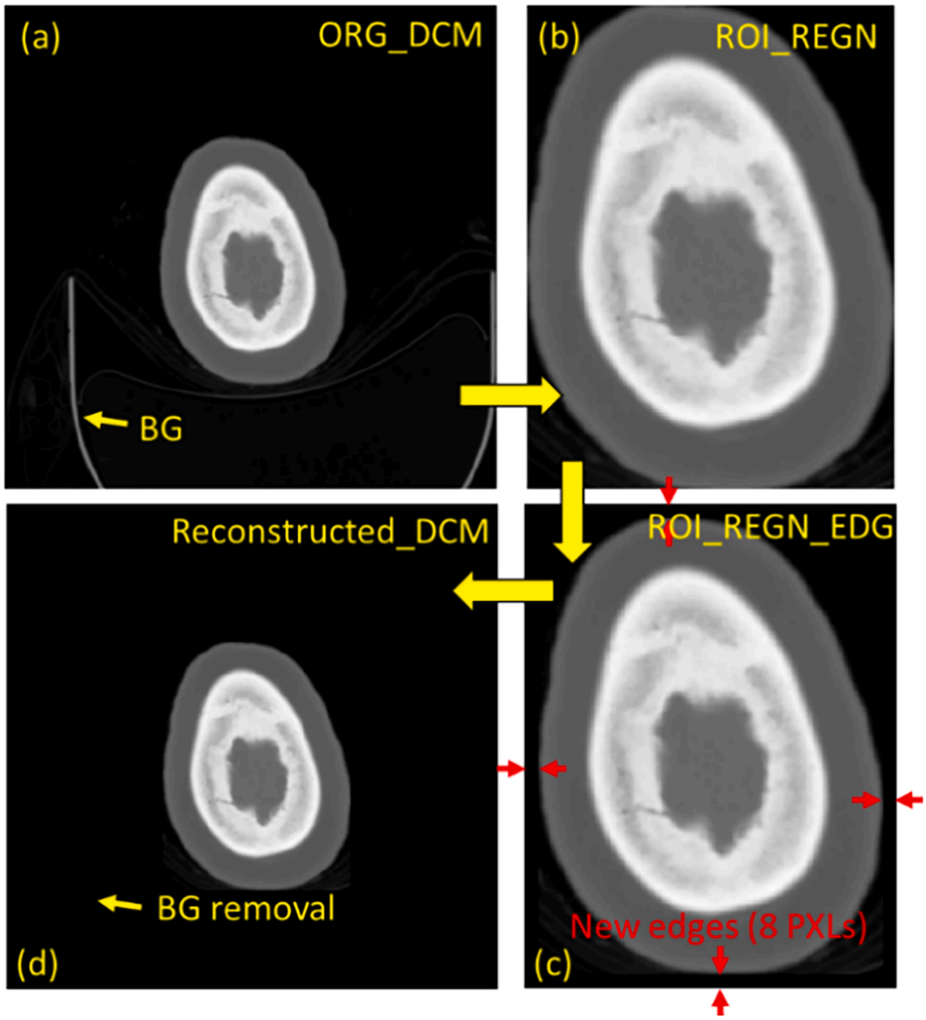

Fig. 7. Improvement of ROI_REGN-based compression of CT and MRI medical images by adding 8-pixels edges. (a) ORG CT image; (b) ROI_REGN image; (c) ROI_REGN image with 8-pixels edges (ROI_REGN_EDG); (d) Reconstructed CT image by JPEGXT_OPT LQ.

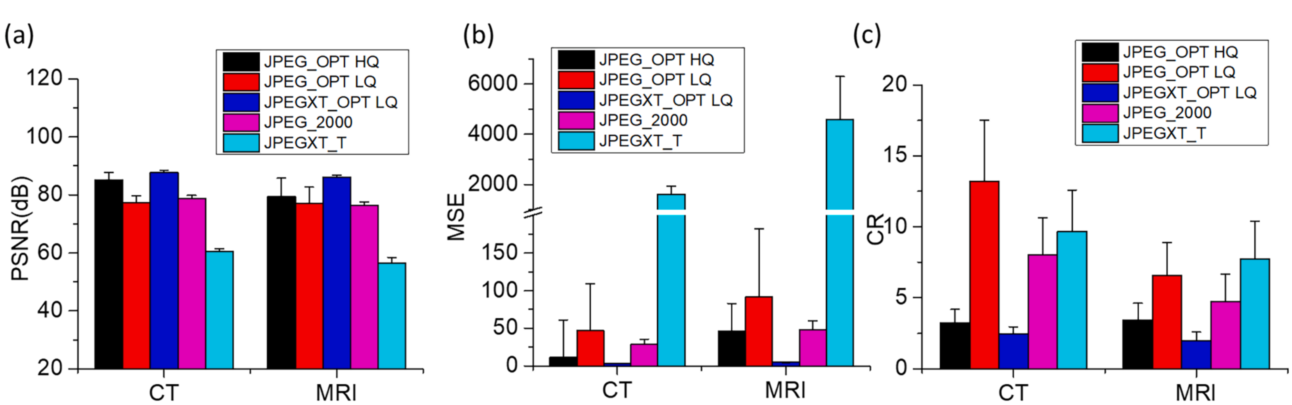

Fig. 8. Evaluation of ROI_REGN_EDG-based compression of CT and MRI images by using JPEG_OPT HQ and JPEG_OPTLQ, JPEGXT_OPT LQ, and the DICOM-recommended methods: JPEGXT_T and JPEG_2000. (a) PSNR; (b) MSE; (c) CR. LQ compression of JPEG_OPT: CT: N = 10, NDP = 1; MRI: N = 50, NDP = 1.

could achieve the highest values (close to 1.0) under both ORG and ROI-based compression, when JPEG_OPT with ROI_REGN_EDG could have over 0.98 MSSIM values. Both of them had a larger MSSIM value than the DICOM-recommended JPEG_2000. JPEGXT_T had the lowest MSSIM values (<0.95) (Fig. 10).

Regarding the PRD evaluation, JPEGXT_OPT still had the lowest image distortions than the other three methods; in particular, ROI_PXL_SORT method could help to decrease the distortions at least three times lower (only 0.05 % in HQ and 0.15 % in LQ) than ORG (only 0.15 % in HQ and 1.3 % in LQ). In JPEG_OPT, both the ORG and ROI_REGN_EDG methods had about 2 % to 3 % distortion rates in CT and MRI images, while JPEG_2000 had a similar distortion rate to JPEG_OPT LQ (Fig. 11). However, JPEGXT_T approach had much larger distortions (over 20 %) than the other three approaches.

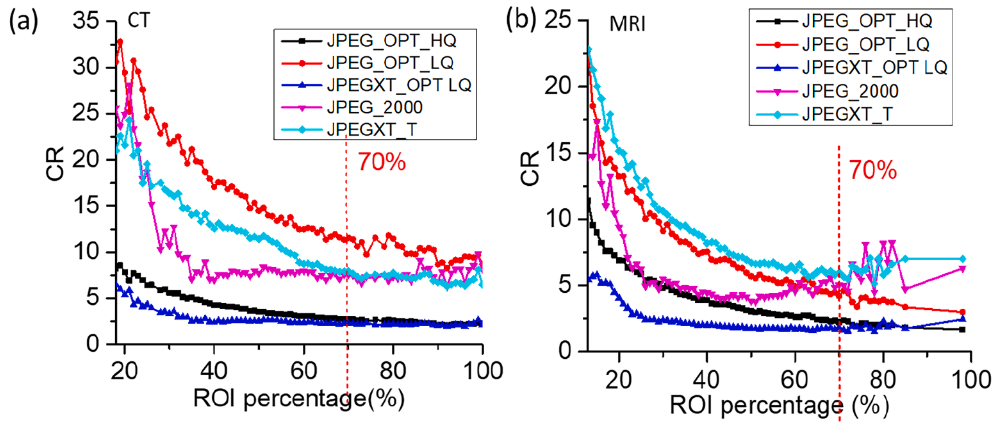

Fig. 9. CR distributions under different ROI percentages by using the ROI_REGN_EDG method under JPEG_OPT, JPEGXT_OPT, and compared to the DICOM-recommended methods: JPEGXT_T, and JPEG_2000. (a) CT; (b) MRI.

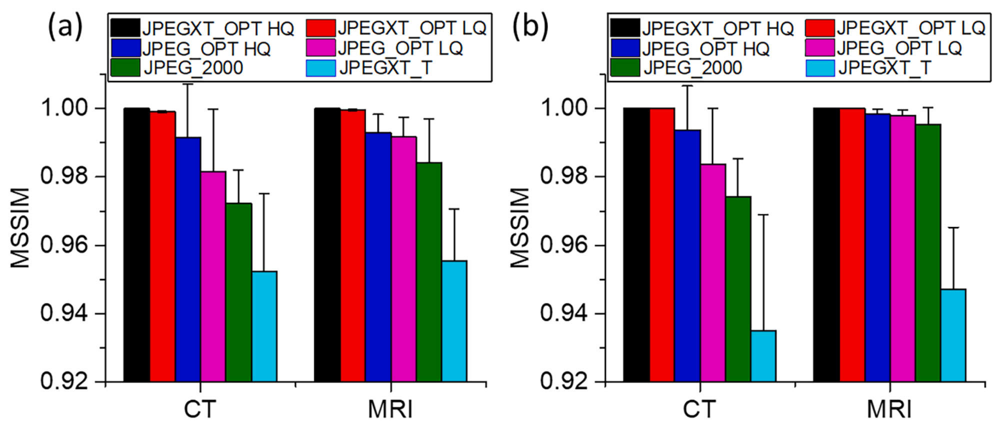

Fig. 10. MSSIM of CT and MRI compression under different JPEG-based approaches. (a) ORG; (b) ROI_PXL-SORT (JPEGXT_OPT) and ROI_REGN_EDG (JPEG_OPT, JPEGXT_T and JPEG_2000).

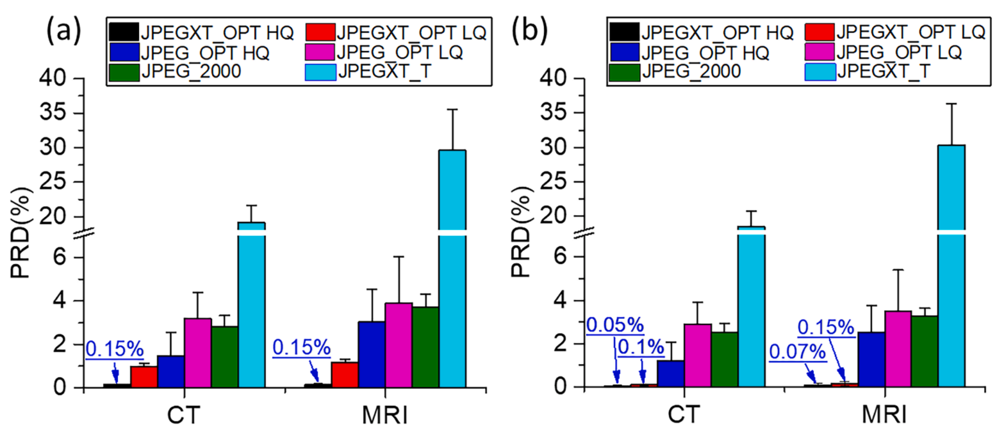

Fig. 11. PDR of CT and MRI compression under different JPEG-based approaches. (a) ORG; (b) ROI_PXL-SORT (JPEGXT_OPT) and ROI_REGN_EDG (JPEG_OPT, JPEGXT_T and JPEG_2000).

A CT image was used to investigate the prediction error images and their corresponding histogram of pixel errors. From the JPEGXT_OPT with ROI_PXL_SORT, we could see that over 98.9 % of pixels had no pixel error (equal to 0) in both HQ and LQ compression. For the JPEG_OPT, over 56 % of the pixels had no pixel errors under ROI_REGN-EDG compression; in the HQ compression, most of the pixel errors were locating the ranges<9, but this ranges increased to over 35 under LQ compression (Fig. 12).

From the prediction error images, almost the entire error images looked kind of dark for the ROI_PXL_SORT, except for some locally bright dots, which means there were almost no compression errors were found from the reconstructed images. Similar results were also found in JPEG_2000 and JPEGXT_T with ROI_PXL_SORT (Fig. S7).

For the JPEG_OPT approach, there were plenty of bright dots (like white noise) distributing in the entire error images, especially under HQ error image that those pixel errors evenly distribute in the whole

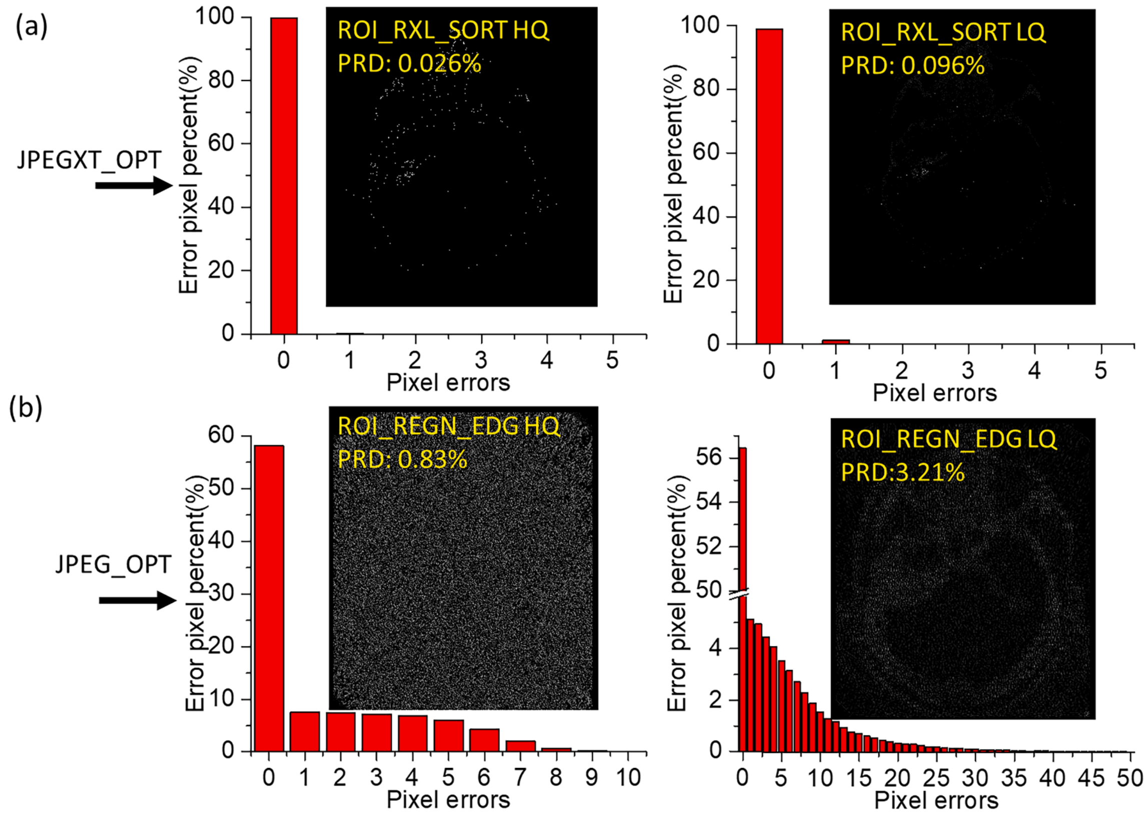

Fig. 12. Prediction error images and their corresponding histogram of the CT image compressed by ROI-based JPEGXT_OPT and JPEG_OPT approaches. (a) JPEGXT_OPT with high and low-quality ROI_PXL_SORT; (b) JPEG_OPT with high and low-quality ROI_REGN_EDG.

anatomical regions. In the error image of JPEG_OPT LQ and JPEG_2000, however, the pixel errors were distributed towards the areas with complicated anatomical structures (Fig. 12). JPEGXT_T with ROI_REGN_EDG had much larger pixel error ranges (up to 80) than the other three methods (JPEGXT_OPT, JPEG_OPT, and JPEG_2000), which cause its larger PRD values (22.15 %).

Although JPEG_OPT had a relatively larger PRD (over 3.21 % under LQ) than that of HQ (PRD = 0.83 %), no visible distortion was found in reconstructed images (Fig. 13b). Compared to JPEG_OPT, the DICOM-recommended JPEGXT_T had much larger distortion rates (>20 %),

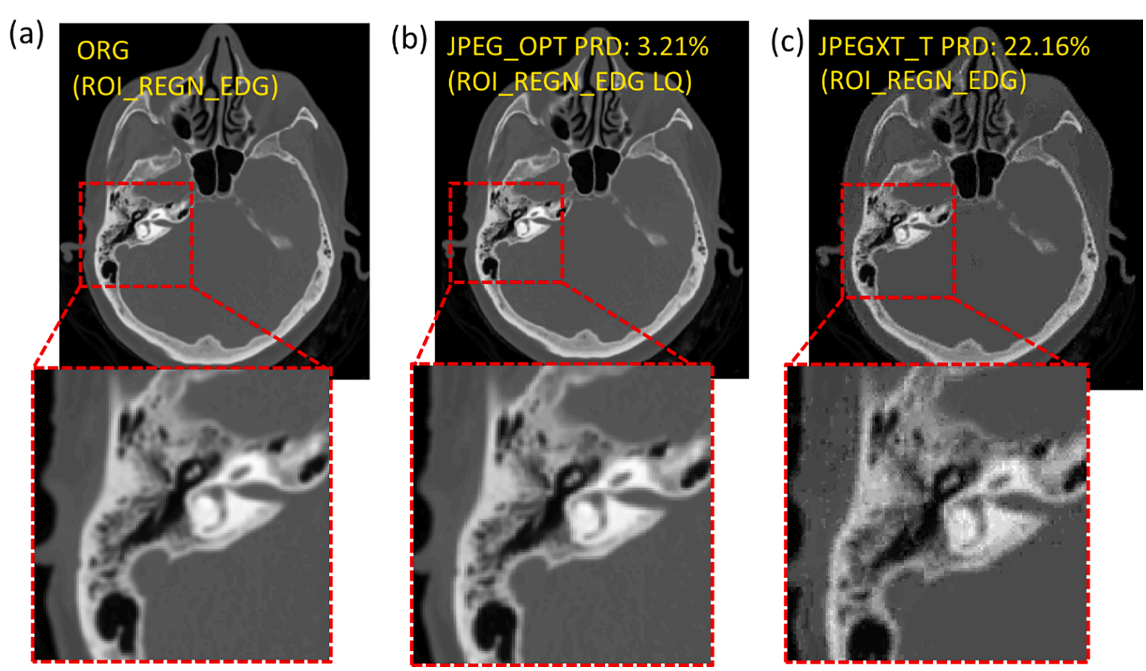

Fig. 13. The distortion evaluation of the reconstructed CT images compressed by JPEG_OPT and JPEGXT_T approaches. (a) ORG CT image; (b) Reconstructed CT image with 3.21% PRD, compressed by JPEG_OPT with ROI_REGN_EDG; (c) Reconstructed CT images with 22.16% PRD, compressed by JPEGXT_T with ROI_REGN_EDG.

and its reconstructed CT images could have about 22.16 % distortions, block boundary artifacts could be observed (Fig. 13c).

4. Discussion

Currently, JPEG-based compression is still widely used in lossy or lossless compression methods for medical applications [2,19]. Our previous JPEGXT_OPT algorithm could achieve lossy or nearly lossless compression of the 16-bit-depth medical images by the control of N and NDP values [21]. In this study, we used more numbers of CT and MRI images to further investigate the influences of ROI percentage on the compression ratio. The results indicate that when compressing entire images, JPEGXT_OPT indeed could achieve higher compression quality (PSNR>=90, MSE < 4.2) than the DICOM-recommended JPEGXT_T (PSNR<=60, MSE > 1000) and JPEG_2000 (PSNR<=80, MSE > 25) methods (Fig. S2). Regarding the compression quality, larger N and NDP values decrease the compression ratio; JPEGXT_T and JPEG_2000 have higher CRs than the JPEGXT_OPT approach.

In the existing studies, most of the new compression algorithms were only tested with a limited amount of images [14,16,26–29], and few studies have systematically presented whether the percentages of ROI occupied in the entire medical images would impact the compression ratio of the compression algorithms. Here, we used 4211 CT and MRI images with different ROI percentages to explore how ROI percentages would have an effect on the compression ratio. From the analysis of CT and MRI datasets, 70 % of CT images and 90 % of MRI images were images with ROI percentages of<70 %, and most of the anatomical regions were ranging from 30 to 70 % ROI percentages. This means plenty of pixels are considered to be background containing useless information on the anatomical structures.

We found that the ROI percentage has an impact on the compression ratio; it is easier to obtain a higher compression ratio under smaller ROI percentages. For JPEGXT_OPT method, ROI_PXL_SORT method had much higher CR than the ORG compression for most ROI percentages (10 % to 90 %). CR could reach over 2.0 (saving over 50 % of space) for the entire datasets and up to 4.0 for ROI percentage<30 %, which is similar or higher than the DICOM-recommended lossless methods [36], and its performance (PSNR and MSE) was much better than the DICOM-recommended JPEGXT_T and JPEG_2000. For lossy JPEG_OPT methods, the 16-bit depth medical image was converted into an 8-bit depth image, and then can be compressed by the DICOM-recommended JPEG algorithm; by optimization of Ns and NDPs, JPEG_OPT with ROI_REGN_EDG achieved a higher compression efficiency (larger PNSR and smaller MSE) than DICOM-recommended JPEGXT_T and JPEG_2000. Similar to JPEGXT_OPT, JPEG_OPT could obtain a higher compression ratio under smaller ROI percentages (CR > 13.0 for CT and CR > 5.0 for MRI under ROI percentage < 70 %).

In our previous study, the lower 8-bit encoding files account for over 90 % of the entire encoding files [21]. Thus, it is very challenging to further increase the compression ratio with JPEGXT_OPT method, even using the ROI method (CR < 5.0). To date, JPEG is still one of the most mainstream approaches for image compression, but it only limits to compress images with 8-bit depth [2,30]. In this study, the JPEG_OPT approach was developed to avoid the impact of lower 8-bit encoding files in JPEGXT_OPT and compress the medical images with over 8-bit depths. Regarding the compression efficiency, JPEG_OPT, especially JPEG_OPT HQ, shows a larger PSNR and smaller MSE than the DICOM-recommended JPEGXT_T and JEPG_2000. There was almost no difference between JPEG_OPT LQ and JPEG_2000, but the CR of JPEG_OPT was larger than JPEG_2000 for both CT and MRI images.

However, lossless compression could ensure no loss of diagnostic information and data fidelity during the image compression and reconstruction, but its current CR is only limited from 2.0 to 3.0 (depending on the images and the methods) [16]. Compared to lossless compression, lossy compression could provide a much higher compression ratio (>10.0) [16]. If using the diagnostic quality of compressed images could be ensured, very little image distortion would be allowed within a certain level [5,37,38].

The topic of using lossy compression in medical images has been long discussed by government organizations, professional societies, etc. [2]. More recently, several professional organizations have given guidelines for using lossy compression in medical images; for instance, the Royal College of Radiologists provided the recommendation of the lossy compression ratio at 5.0 for CT, 10.0 for ultrasound, 20.0 for mammography or Canadian Association of Radiologists recommends that the maximum lossy compression ratios of JPEG are no>15.0 for CT and 24.0 for MRI [2,23,24]. However, there is still a lack of legal standards for radiological images, and no specific standards or guidelines are provided to evaluate how many image distortions for lossy algorithms could be allowed to guarantee diagnostic quality [37–39].

In this study, including PSNR, MSE, and CR, more evaluation parameters (MSSIM and PRD) are employed to evaluate the distortions because of using lossy JPEG_OPT. From the distortion analysis, our two methods also showed a lower distortion than the DICOM-recommended JPEGXT_T and JPEG_2000. JPEGXT_OPT had a very low PRD (<0.02 %) and high MSSIM (>0.9999). For JPEG_OPT, it also exhibits outstanding MSSIM (>0.98) which means there were almost no changes in luminance, contrast, and structure between the original and reconstructed CT and MRI images. only about 3 % PDR was found in JPEG_OPT LQ (similar to JPEG_2000), and no distortion was observed from the reconstructed images (CT image in Fig. 13).

Compared to MSSIM, PRD seems to be more sensitive to the distortion of reconstructed images. For the DICOM-recommended JPEGXT_T, its MSSIM was ranging from 0.93 to 0.95 that is closed to JPEG_2000, but the PDR (over 20 %) of the DICOM-recommended JPEGXT_T was much larger than our two methods and JPEG_2000 (around 3 %); from the reconstructed CT image (Fig. 13), block boundary artifacts were clearly observed under JEPGXT_T with PDR = 22.16 %.

Overall, by adjusting the amplification of DCT coefficients, JPEG_OPT could obtain high-quality compression of medical images without significant loss of important diagnostic; our method can obtain a higher compression efficiency than DICOM-recommended JPEG 2000 and JPEGXT_T without significant distortions: over 10.0 for the whole ROI percentages and up to 37.0 for the small ROI percentage (around 20 %). For the distortion analysis, MSSIM can be in combination with PRD for the distortion evaluation, in which MSSIM could be used to evaluated structural distortion from multiple scales, while PRD could give a quantitative evaluation of the distortion.

In addition, more and more new nearly-lossless or lossy compression methods (including both JPEG-based and other methods) have been reported for the application of medical imaging recently [40]. For instance, Vempati Krishna and his co-worker reported ROI-based binary-plane coding for MRI, and it could achieve PSNR over 43.0 and SSIM > 0.97 [29]; M. M. S. Rani and P. Chitra represented a hybrid method based on Haar wavelet transform and particle swarm optimization technique that had around 43.0 in PSNR, 3.24 in MSE, 5.2 in CR, about 0.96 in MSSIM [41]. Meanwhile, some of the researchers also attempted to develop ROI-based hybrid approaches that could achieve better compression performances. For example, Lakshminarayana M., and Mrinal S. developed the combination of both lossless (*JPEG-2000 + Huffman + Run length*) for ROI regions and lossy (*Compressive Sensing*) methods for non-ROI regions and their new framework achieved about 8.60 MSE, 41.5 in PSNR 5.5 in CR for ROI regions, but its MSE increased over 208.8 (PSNR dropped to 34.9) in full image [42]. However, the above new approaches still have relative lower compression efficiency than our two approaches. More importantly, most of them only used the limited numbers of medical images to test their compression efficiency.

Finally, deep learning is emerging as a new technique for medical image compression. Although some groups reported the new deep learning approach could achieve about 15 % higher compression ratio than conventional methods[43], they may still have the problems of higher MSE, lower PSNR, and loss of granular details [44,45]. From our results, both of our two methods could achieve nearly-lossless and lossy image compressions. In particular, the lossy compression JPEG-OPT could obtain relatively high PSNR and low MSE, and have almost no distinct image distortion (about 3.21 % PRD).

However, there are still some limitations in this study. First, the Th_value is playing a key role in the CT and MRI binarization, and this study uses maximum pixels with two different percentages to determine the thresholds between the ROI and BG. Although this method works efficiently for CT and MRI images used in this study, more imaging data or a more efficient method needs to be explored to obtain a better ROI and BG segmentation. Secondly, although our study used more numbers of CT and MRI images to test our algorithms than most of the existing studies[5,16,26,46], more image data with different imaging conditions and more imaging modalities are required to further test our approaches. Finally, even though our methods have been compared with two DICOM-recommended standard JPEG-based approaches, JPEG_XT and JPEG_2000, and both could achieve better compression efficiency, more methods (like DICOM RLE Image Compression and deep learning-based algorithms), rather than JPEG-based methods, need to be further tested.

5. Conclusions

In this study, by using the anatomical regions as ROI, we tested its compression efficiency for JPEGXT_OPT and JPEG_OPT, and investigated the influences of different ROI percentages on the compression ratio. We found that JPEGXT_OPT with ROI_PXL_SORT could perform nearly-lossless compression of medical images; ROI percentages have an effect on the compression ratio: JPEGXT_OPT could obtain a higher compression ratio (up to 4.5) under smaller ROI percentages (10 to 30 %), while only around 1.2 under the entire medical images (90–100 %). To further increase CR, JPEG_OPT was developed for the lossy compression of medical images. The compression ratio could greatly be improved: CR > 20.0 for both CT and MRI images under small ROI percentages (10 %- 30 %), and CR was still>10.0 for CT and 5.0 for MRI under large ROI percentages (>90 %), which is higher than JPEG_2000.

From the distortion analysis, ROI-based JPEGXT_OPT had a very low PRD (<0.02 %) and high MSSIM (>0.9999). Although there was about 3.0 % distortion (PRD = 3.0 %) found in JPEG_OPT compression, no obvious distortion was observed from the reconstructed image; MSSIM (>0.98) further indicated there were almost no changes in luminance, contrast, and structure between the original and reconstructed image. Both of our methods exhibited better compression quality and lower distortion than the DICOM-recommended JPEGXT_T and JPEG_2000, especially block boundary effects found in JPEGXT_T. Therefore, by adjusting the amplification of DCT coefficients, our methods could achieve nearly-lossless-to-lossy compression of medical images, and JPEG_OPT could perform high-quality lossy compression of medical images without significant loss of important diagnostic information.

Declaration of Competing Interest

The authors declare that they have no known competing financial interests or personal relationships that could have appeared to influence the work reported in this paper.

Data availability

Data will be made available on request.

Acknowledgments

We thank Dr. Shaomian Yao from the Department of Comparative Biomedical Science, LSU for his great review and suggestions of this manuscript. This research was supported by Louisiana State University Faculty Research Grants (009875, 010215), LSU Leveraging Innovation for Technology Transfer (LIFT2) Grant (LSU-2021-LIFT-009, LSU-2020-LIFT-008), LSU Collaborative Cancer Research Initiative (010163), Louisiana Board of Regents Grant (LEQSF (2018-21)-RD-A-09), NSF CAREER award (2046929).

Appendix A. Supplementary data

Supplementary data to this article can be found online at https://doi.org/10.1016/j.bspc.2023.104711.

References

[1] R. Duszak, Medical imaging: is the growth boom over, Neiman Report, Harvey L. Neiman Health Policy Institute, Reston, Virginia, (2012).
[2] F. Liu, M. Hernandez-Cabronero, V. Sanchez, M.W. Marcellin, A. Bilgin, The Current Role of Image Compression Standards in Medical Imaging, Information (Basel) 8 (2017) 131.
[3] J. Watanabe, M. Ota, Y. Suwa, A. Ishibe, H. Masui, K. Nagahori, Evaluation of lymph flow patterns in splenic flexural colon cancers using laparoscopic real-time indocyanine green fluorescence imaging, International journal of colorectal disease 32 (2017) 201–207.
[4] J. Xu, D.A. Kooby, S. Nie, Nanofluorophore Assisted Fluorescence Image-guided Cancer Surgery, J Med-Clin Res & Rev 2 (2018) 1–3.
[5] X. Song, Q. Huang, S. Chang, J. He, H. Wang, Novel Near-Lossless Compression Algorithm for Medical Sequence Images with Adaptive Block-Based Spatial Prediction, J Digit Imaging 29 (2016) 706–715.
[6] Z. Li, W. Zaid, T. Hartzler, A. Ramos, M.L. Osborn, Y. Li, S. Yao, J. Xu, Indocyanine green-assisted dental imaging in the first and second near-infrared windows as compared with X-ray imaging, Ann N Y Acad Sci 1448 (2019) 42–51.
[7] Z. Li, Z. Li, Y. Holamoge, W. Zaid, M. Osborn, S. Bhatta, A. Jeyaseelan, Y. Li, S. Yao, J. Xu, Mouthwash to deliver indocyanine green for near infrared dental fluorescence imaging, IEEE Journal of Selected Topics in Quantum Electronics (2020).
[8] Z. Li, T. Hartzler, A. Ramos, M.L. Osborn, Y. Li, S. Yao, J. Xu, Optimal imaging windows of indocyanine green-assisted near-infrared dental imaging with rat model and its comparison to X-ray imaging, J Biophotonics 13 (2020) e201960232.
[9] Z. Li, S. Yao, J. Xu, Indocyanine-green-assisted near-infrared dental imaging - the feasibility of in vivo imaging and the optimization of imaging conditions, Scientific reports 9 (2019) 8238.
[10] J. Janet, D. Mohandass, S. Meenalosini, Lossless compression techniques for Medical images in Telemedicine, Advances in Telemedicine Technologies, Enabling Factors, Scenario (2011) 111–130.
[11] S. Saha, Image compression—from DCT to wavelets: a review, Crossroads 6 (2000) 12–21.
[12] M.J. Weinberger, G. Seroussi, G. Sapiro, LOCO-I: A low complexity, context-based, lossless image compression algorithm, Data Compression Conference, 1996. DCC'96. Proceedings, IEEE, 1996, pp. 140-149.
[13] T. Kumar, R. Kumar, Medical image compression using hybrid techniques of DWT, DCT and Huffman coding, International Journal of Innovative research In Electrical, Electronics, Instrumentation and control engineering 3 (2015) 54–60.
[14] Z. Zuo, X. Lan, L. Deng, S. Yao, X. Wang, An improved medical image compression technique with lossless region of interest, Optik 126 (2015) 2825–2831.
[15] P.G. Tahoces, J.R. Varela, M.J. Lado, M. Souto, Image compression: Maxshift ROI encoding options in JPEG2000, Computer Vision and Image Understanding 109 (2008) 139–145.
[16] Y. Lalitha, M. Latte, Lossless and lossy compression of DICOM images with scalable ROI, International Journal of Computer Science and Network, Security 10 (2010) 276–281.
[17] V. Radha, A comparative study on ROI-based lossy compression techniques for compressing medical images, Proceedings of the World Congress on Engineering and Computer Science, 2011.
[18] D. Yee, S. Soltaninejad, D. Hazarika, G. Mbuyi, R. Barnwal, A. Basu, Medical image compression based on region of interest using better portable graphics (BPG), 2017 IEEE international conference on systems, man, and cybernetics (SMC), IEEE, 2017, pp. 216-221.
[19] P. Sreenivasulu, S. Varadarajan, An Efficient Lossless ROI Image Compression Using Wavelet-Based Modified Region Growing Algorithm, Journal of Intelligent Systems 29 (2018) 1063–1078.
[20] A. Zimbico, F. Schneider, J. Maia, Comparative study of the performance of the JPEG algorithm using optimized quantization matrices for ultrasound image compression, Biosignals and Biorobotics Conference (2014): Biosignals and Robotics for Better and Safer Living (BRC), 5th ISSNIP-IEEE, IEEE, 2014, pp. 1-6.
[21] Z. Li, A. Ramos, Z. Li, M.L. Osborn, X. Li, Y. Li, S. Yao, J. Xu, An optimized JPEG-XT-based algorithm for the lossy and lossless compression of 16-bit depth medical image, Biomedical Signal Processing and Control 64 (2021), 102306.
[22] G.K. Anastassopoulos, A. Skodras, JPEG2000 ROI coding in medical imaging applications, Proc. 2nd IASTED Int, Conf. on Visualisation, Imaging and Image Processing (VIIP2002), Citeseer (2002) 783–788.
[23] R.C.o. Radiologists, The Adoption of Lossy Image Data Compression for the Purpose of Clinical Interpretation, Royal College of Radiologists, 2008.
[24] C.A.o. Radiologists, CAR Standards for Irreversible Compression in Digital Diagnostic Imaging within Radiology, Canadian Association of Radiologists, 2011.

[25] D.S. Committee, DICOM PS3.5 2018e - Data Structures and Encoding, in: N.E.M. Association (Ed.), DICOM Standards Committee, pp. 121-125.
[26] V.K. Bairagi, A.M. Sapkal, ROI-based DICOM image compression for telemedicine, Sadhana 38 (2013) 123–131.
[27] A. Kaur, M. Goyal, Roi based image compression of medical images, International Journal of Computer Science Trends and Technology (2014) 2347–8578.
[28] G.U.V. Selvi, R. Nadarajan, CT and MRI image compression using wavelet-based contourlet transform and binary array technique, Journal of Real-Time Image Processing 13 (2017) 261–272.
[29] V. Krishna, V.P.C. Rao, Region based medical image compression with Binary Plane Coding, ARPN Journal of Engineering and Applied Sciences 12 (2017).
[30] G. Hudson, A. Léger, B. Niss, I. Sebestyén, J. Vaaben, JPEG-1 standard 25 years: past, present, and future reasons for a success, Journal of Electronic Imaging 27 (2018), 040901.
[31] K. Clark, B. Vendt, K. Smith, J. Freymann, J. Kirby, P. Koppel, S. Moore, S. Phillips, D. Maffitt, M. Pringle, The Cancer Imaging Archive (TCIA): maintaining and operating a public information repository, Journal of digital imaging 26 (2013) 1045–1057.
[32] N.C.I.C.P.T.A. Consortium, Radiology Data from the Clinical Proteomic Tumor Analysis Consortium Glioblastoma Multiforme [CPTAC-GBM] collection, The Cancer Imaging Archive (2018).
[33] P. Kumar, A. Parmar, Versatile approaches for medical image compression: A review, Procedia Computer Science 167 (2020) 1380–1389.
[34] Z. Wang, E.P. Simoncelli, A.C. Bovik, Multiscale structural similarity for image quality assessment, The Thrity-Seventh Asilomar Conference on Signals, Systems & Computers, 2003, Ieee, 2003, pp. 1398-1402.
[35] G.P. Renieblas, A.T. Nogues, A.M. Gonzalez, N. Gomez-Leon, E.G. Del Castillo, Structural similarity index family for image quality assessment in radiological images, J Med Imaging (Bellingham) 4 (2017), 035501.
[36] J. Kivijarvi, T. Ojala, T. Kaukoranta, A. Kuba, L. Nyul, O. Nevalainen, A comparison of lossless compression methods for medical images, Comput Med Imaging Graph 22 (1998) 323–339.
[37] A. Miguel, E. Riskin, R. Ladner, D. Barney, Near-lossless and lossy compression of imaging spectrometer data: comparison of information extraction performance, Signal, Image and Video Processing 6 (2012) 597–611.
[38] K. Chen, T.V. Ramabadran, Near-lossless compression of medical images through entropy-coded DPCM, IEEE Transactions on Medical Imaging 13 (1994) 538–548.
[39] M.J. Gormish, E.L. Schwartz, A.F. Keith, M.P. Boliek, A. Zandi, Lossless and nearly lossless compression for high-quality images, very High resolution and Quality Imaging II, International Society for Optics and Photonics (1997) 62–70.
[40] S. Ab Aziz, S.M. Sam, N. Mohamed, S.M. Daud, S.Z.A. Rashid, H. Abas, M.F. Yusof, R.A. Dziyauddin, A review on region of interest-based hybrid medical image compression algorithms, TELKOMNIKA 18 (2020) 1650–1657. Telecommunication Computing Electronics and Control),.
[41] M.M.S. Rani, P. Chitra, A hybrid medical image coding method based on haar wavelet transform and particle swarm optimization technique, International Journal of Pure and Applied Mathematics 118 (2018) 3056–3067.
[42] M. Lakshminarayana, M. Sarvagya, MICCS: A novel framework for medical image compression using compressive sensing, International Journal of Electrical and Computer Engineering (IJECE) 8 (2018) 2818–2828.
[43] O.H. Nagoor, J. Whittle, J. Deng, B. Mora, M.W. Jones, MedZip: 3D medical images lossless compressor using recurrent neural network (LSTM), 2020 25th International Conference on Pattern Recognition (ICPR), IEEE, 2021, pp. 2874-2881.
[44] S.S. Tamboli, R. Butta, T.S. Jadhav, A. Bhatt, Optimized active contor segmentation model for medical image compression, Biomedical Signal Processing and Control 80 (2023), 104244.
[45] K.J. Chung, R. Souza, R. Frayne, Restoration of lossy JPEG-compressed brain MR images using cross-domain neural networks, IEEE Signal Processing Letters 27 (2019) 141–145.
[46] N.R.A. D.VIJENDRA BABU, Wavelet Based Medical Image Compression Using ROI EZW, International Journal of Recent Trends in Engineering, 1 (2009).